CONTROL SYSTEMS AND DYNAMICS OF CONE-SHAPED MAGNETIC BEARINGS ACTUATED BY FIVE ELECTROMAGNETS

Satoru Fukata
Department of Energy and Mechanical Engineering, Kyushu University, Fukuoka, Japan.
Shinya Matsuoka
Graduate School, Division of Engineering, Kyushu University, Fukuoka, Japan.

ABSTRACT
A five-axis control system actuating five electromagnets is considered for a symmetric magnetic bearing system composed of six electromagnets whose pole faces are in the shape of a cone to combine radial bearings with a thrust bearing. The extra one electromagnet is used only as a bias actuator. The square-root compensation is applied to linearize the control force. The linearized model is obtained with the five resultant inputs which are given by the combination of actual inputs of the electromagnets. The control system is realized with the actual inputs assigned to generate these resultant inputs, the control inputs into the individual control axes. A little modification of the assignment of the actual inputs leads to a simpler form that gives some interaction. Experimental data are obtained for frequency responses of the control systems and transient responses to impact to show the characteristics of the system.

1. INTRODUCTION

Active magnetic bearing systems are usually constructed with electromagnets (EMs) twice the control axes: for example, ten for the five-axis control. The use of such a large number of EMs is unfavorable to the cost and the reliability of the systems. One approach to reducing EMs is to combine radial bearings with a thrust bearing by shaping the magnet pole faces in a cone. This bearing system may be constructed with eight electromagnets [1]-[3] for five-axis control in practical use. This system can be realized also with six EMs[4]; however, since the control forces are interactive, the design of the control system becomes complicated.

The cone-shaped magnetic bearing system with six EMs has only one extra EM for control; the least number of actuators necessary for five-axis control is theoretically five. In addition, this extra one is useful for the push-pull control. Thus, six EMs may be the most reasonable set for reducing EMs in the five-axis-control bearing systems. Keeping this fact in mind, we try to use five EMs in the control for the further improvement in cost reduction and reliability increase. The extra one is assigned for a bias actuator so that its dynamic characteristics are not important, or instead a permanent magnet may be used.

The cone-shaped bearing system considered here is symmetric in structure, supporting a symmetric rotor in the horizontal direction. The magnet cores are made of solid steel for both stator and rotor for simplicity in manufacturing. All the electromagnets including the one used for the bias actuator have the same specification.

The control system is designed so that the resultant control inputs might be decoupled into the five control axes, based on the linearized model. Since the control action is not push-pull but individual with a pair of electromagnets in three control axes, the square-root compensation is applied to linearize the control forces. A little modification of the control input scheme leads to a simpler form that gives some interaction. Experimental data are obtained for frequency responses of the control systems and the transient responses to impact into the rotor to show the characteristics of the system.

2. CONE-SHAPED BEARING SYSTEM WITH SIX ELECTROMAGNETS

Figure 1 shows the mechanical part of the cone-shaped magnetic bearing system which is composed of six electromagnets (EMs) and is symmetric in structure, supporting a symmetric rotor in the horizontal direction. In the figure, ③ and ⑤ are magnet cores of the stator and the rotor, respectively; both are made of solid steel. ① and ② are displacement sensors of eddy current type and ④ is the target of the radial sensors. ⑥ is an air turbine to

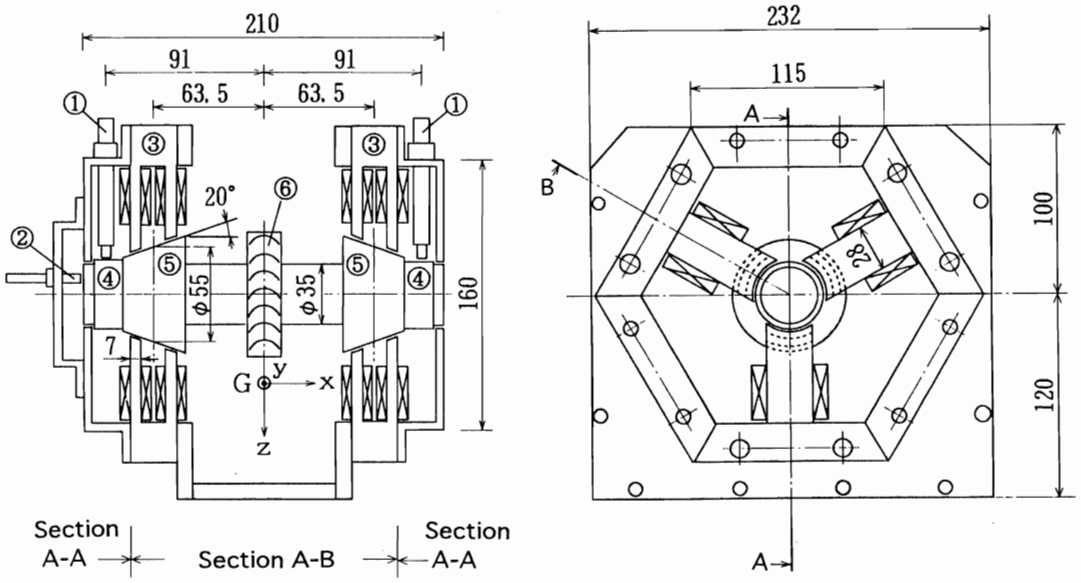

FIGURE 1. Cone-Shaped Bearings Composed of Six Electromagnets

drive the rotor. The air gap is the length of 0.5mm.

The EMs are numbered by ij as follows: The first i is used for the bearings: "1" for the left-hand side, and "2" for the right-hand side. The second j is for the EMs: the lower side by 1, and the upper side by 2 and 3 in the positive and negative sides, respectively, of the y direction. The lower-side EM of the right-hand side bearing, numbered by 21, gives only a bias force. In the below, variables associated with each individual EM are shown with subscript of these numbers.

To describe the rotor motion, we set the x, y and z axes, originated at the center of gravity of the rotor in the steady state, into the axial, radially horizontal and vertical directions, respectively.

3. LINEARIZED MODEL

3.1 Notations

The notations are summarized in the followings.

Variables:

x : axial displacement of rotor

y, z : radial displacements of translatory motion

y_R, z_R : displacements of conical motion, measured at the center of bearing

q_x', ... : variables used to decribe control force

d_x,... : disturbance forces except for magnetic force

u_x,... : control inputs

v_{ij} : incremental input to be given

E_{ij} : absolute input of electromagnet ij

Data:

A : area of magnet-core face of stator (2.1 cm^2)

b : gain of power amplifier (0.97 A/V)

D : diameter of rotor at the center of bearing (55 mm)

I_{10} : bias current of lower-side magnet coil (1.0 A)

I_{20} : bias current of upper-side magnet coil (1.6 A)

L : distance between the centers of rotor and bearing (63.5mm)

l_{0S} : air gap length with the resistance in magnet core (0.52mm)

m : rotor mass (2.74 kg)

m_R : equivalent mass of conical motion (2.31 kg)

m_P : equivalent mass with gyroscopic effect (0.228 kg)

N : turns of magnet coil (200)

α : half angle of cone (20 deg.)

β : angle of pole face in the radial direction (0 deg)

ω : angular velocity of rotor (0 rad/s)

$$k_{Fj} = \left[\frac{\mu_0 A}{4}\left(\frac{N}{l_{0S}}\right)^2\right]_j, \quad a_{0j}' = \frac{2I_{j0}^{\,2}}{l_{0S}}, \quad j = 1,2$$

$$c_{F12} = \frac{k_{F2}}{k_{F1}}, \quad c_{F12a} = c_{F12}\frac{a_{02}'}{a_{01}'} = c_{F12}\left(\frac{I_{20}}{I_{10}}\right)^2$$

$$c_1 = \cos\alpha\cos\beta$$

$$p = 1 - \frac{D}{2L}\tan\alpha, \quad p_1 = 1 - \frac{D}{2L}\tan\alpha\cos\beta$$

$$p_c = 1 - \frac{D}{4L}\tan\alpha, \quad p_s = 1 - \frac{\sqrt{3}D}{4L}\tan\alpha$$

$$K_{Fx}' = 6k_{F1}\sin\alpha$$

$$K_{Fy}' = 2\sqrt{3}k_{F2}c_1, \quad K_{Fz}' = 4k_{F1}c_1$$

$$a_x' = (1/3)a_{01}'(1 + 2c_{F12a})\sin\alpha$$

$$a_{xzR}' = (1/3)a_{01}'(p_1 - p_c c_{F12a})\,c_1$$

$$a_y' = \sqrt{3}/2)a_{02}'\,c_1, \quad a_{yR}' = p_s a_y'$$

$$a_z' = \frac{1}{2}a_{01}'\left(1 + \frac{1}{2}c_{F12a}\right)c_1$$

$$a_{zR}' = \frac{1}{2} a_{01}' \left(p_1 + \frac{1}{2} p_c c_{F12a} \right) c_1$$

$$a_{zRx}' = (1/2) a_{01}' (1 - c_{F12a}) \sin\alpha$$

3.2 Linearized Model of Magnetic Force

Since electromagnet (EM) 21 does not act in control, the control action is not push-pull, but single action at least for the vertical direction in the right-hand side bearing. The single action causes the nonlinear effects of the magnetic force so that it might be desirable to introduce the square-root compensation for the linearization. The number of the compensation necessary is not clear in this stage, and so we consider this compensation for all the EMs, for simplicity of analysis.

In describing the dynamic characteristics of the EMs, we adopt a simple model presented in [2], considering the first-order effect of eddy currents in solid cores without saturation of magnetic flux. We write the *absolute input*, E, of the power amplifier of an ME as

$$E = E_0 + e \tag{1}$$

where E_0 is a bias input and e is the increment. With this increment, the incremental magnetic force, f, may be expressed by the linearized model as follows[2]:

$$f = 2k_F I_0 q\,,$$

$$T_2\ddot{q} + T_1\dot{q} + q + I_0(T_e\dot{k}_l + k_l) = b(T_e\dot{e} + e) \tag{2}$$

where k_F is a constant, I_0 is a bias coil-current, k_l is the incremental ratio of air-gap length, and T_2, T_1 and T_e are time constants.

To linearize the magnetic force generated by a single ME, we apply the square-root operation as

$$E = \sqrt{V_0 + v} \tag{3}$$

where V_0 is a bias input and v is the increment to be given, *actual input*. If the increment is sufficiently small, then, we have the relations

$$e = \frac{1}{2\sqrt{V_0}} v, \quad \sqrt{V_0} = E_0 = \frac{I_0}{b} \tag{4}$$

With the increment v, eq.(2) is written as follows:

$$f = k_F q' \tag{5a}$$

$$T_2\ddot{q}' + T_1\dot{q}' + q' + 2I_0^{\,2}(T_e\dot{k}_l + k_l) = b^2(T_e\dot{v} + v) \tag{5b}$$

This result may be obtained directly from the original nonlinear model [2]. For simplicity, we write eq.(5b) as

$$g_{21}(D)q' + 2I_0^{\,2}k_l = b^2 v \tag{5c}$$

with the operator defined by

$$g_{21}(D) = \frac{T_2D^2 + T_1D + 1}{T_eD + 1} \tag{6}$$

where D is the differential operator.

3.3 Linearized Equations of Rotor Motion

For the symmetric bearing system with the same dynamic characteristics of the electromagnets, the linearized equations of rotor motion are obtained in [4] with the magnetic force model of eq.(2) (push-pull control action). Considering the difference between the two models, with eq. (5) we obtain the following equations.

$$m\ddot{x} = K_{Fx}' q_x' + d_x\,,$$

$$g_{21}(D)q_x' - a_x' x - a_{xzR}' z_R = b^2 v_x \tag{7}$$

$$m\ddot{y} = K_{Fy}' q_y' + d_y\,,$$

$$g_{21}(D)q_y' - a_y' y = b^2 v_y \tag{8}$$

$$m_R\ddot{y}_R + m_P\omega\dot{z}_R = pK_{Fy}' q_{yR}' + d_{yR}\,,$$

$$g_{21}(D)q_{yR}' - a_{yR}' y_R = b^2 v_{yR} \tag{9}$$

$$m\ddot{z} = K_{Fz}' q_z' + d_z\,,$$

$$g_{21}(D)q_z' - a_z' z = b^2 v_z \tag{10}$$

$$m_R\ddot{z}_R - m_P\omega\dot{y}_R = pK_{Fz}' q_{zR}' + d_{zR}\,,$$

$$g_{21}(D)q_{zR}' - a_{zR}' z_R - a_{zRx}' x = b^2 v_{zR} \tag{11}$$

where the *resultant input* variables are given by the actual inputs as follows:

$$6v_x = -v_{11} + c_{F12}(-v_{123} + v_{223}) \tag{12}$$

$$4v_y = (v_{12} - v_{13}) + (v_{22} - v_{23}) \tag{13}$$

$$4v_{yR} = -(v_{12} - v_{13}) + (v_{22} - v_{23}) \tag{14}$$

$$4v_z = v_{11} + (c_{F12}/2)(-v_{123} - v_{223}) \tag{15}$$

$$4v_{zR} = -v_{11} + (c_{F12}/2)(v_{123} - v_{223}) \tag{16}$$

where

$$v_{123} = v_{12} + v_{13}, \quad v_{223} = v_{22} + v_{23} \tag{17}$$

In the above model, except for the gyroscopic effects, only the conical motion in the vertical direction and the axial motion interact each other through their displacements, and the other motions are independent of each other. This suggests the possibility of an approximate decoupling control for the former two motions and of a decoupling control for the other motions.

4. DECOUPLING OF CONTROL INPUTS

The actual inputs are obtained by the solution of the relations (12)-(16) as follows:

$$v_{11} = -c_{F12}[u_x + (4/3)u_{zR}] \tag{18}$$

$$v_{12} = -u_{zx} + u_{y1}, \quad v_{13} = -u_{zx} - u_{y1} \tag{19}$$

$$v_{22} = -u_{z2} + u_{y2}, \quad v_{23} = -u_{z2} - u_{y2} \tag{20}$$

where, for simplicity, we used the new variables as

$$u_x = (2/c_{F12})v_x \tag{21}$$

$$u_z = (2/c_{F12})v_z, \quad u_{zR} = (2/c_{F12})v_{zR} \tag{22}$$

$$u_y = v_y, \quad u_{yR} = v_{yR} \tag{23}$$

$$u_{zx} = u_x + u_z + u_{zR}/3 \tag{24}$$

$$u_{y1} = u_y - u_{yR}, \quad u_{y2} = u_y + u_{yR} \tag{25}$$

$$u_{z2} = u_z + u_{zR} \tag{26}$$

Figure 2 shows the control input system with the assignment of the actual inputs, eqs.(18)-(20), where the factors are given by $c_F = c_{F12} = 1$ and $k = 1/3$. The figure makes it clear that the control action is

(1) single action for x and z axes,

(2) almost single action for z_R axis, and

(3) push-pull action for y and y_R axes.

Noting (3), we may save the two square-root operators as shown in Fig. 3, where the new resultant inputs are defined for the horizontal motion by

$$u_y' = (b/2I_{20})v_y, \qquad u_{yR}' = (b/2I_{20})v_{yR} \tag{27}$$

The resultant form of the linearized model is given by eqs. (7)-(11) with eqs. (21), (22) and either eq. (23) or (27). We can derive the same equations as in [4] for the horizontal direction by substituting eq. (27) into eqs. (8) and (9).

Incidentally, following back the input relations, we can understand the role of the factors c_F and k in Figs. 2 and 3: c_F separates the translatory and conical control inputs, and k keeps the conical control input off the axial control input[5].

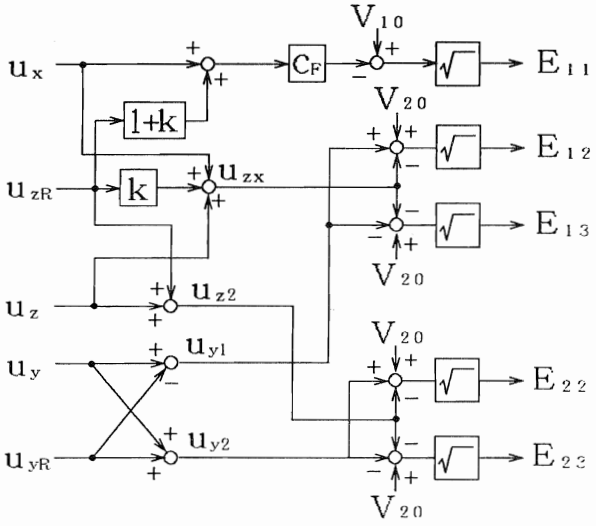

FIGURE 2. Control Input System

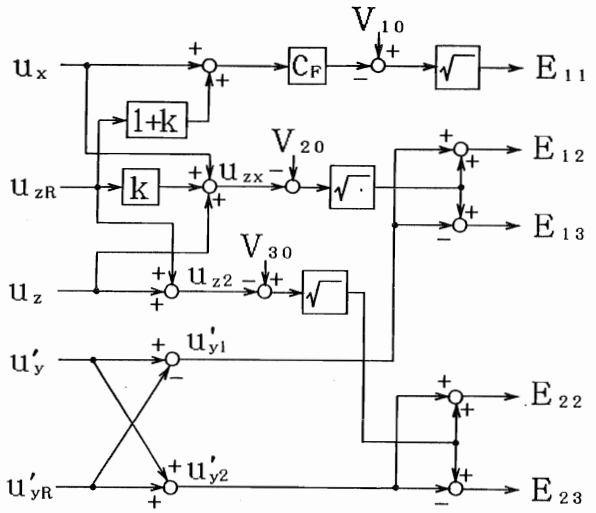

FIGURE 3. Modified Control Input System

5. EXPERIMENTAL RESULTS

The control system was realized with analog circuits. The bias currents of the electromagnets (EMs) are 1.0A and 1.6 A in the lower two and the upper four, respectively. These bias currents give the forces of about 9N and 22N, respectively, theoretically. The absolute inputs into the power amplifiers of the EMs, E_{ij}, were restricted within 0 and 4 V ($0 \leqq E_{ij} \leqq 4$V); the corresponding statical currents are 0 and 4A, respectively. The gain of the displacement sensor is 10 V/mm for the axial and translatory motions, and 14.3 V/mm for the conical motions.

We adopt a PID compensation of single variable, and give the control input in the Laplace transform as

$$U(s) = -G_C(s)X(s) + U_0(s) \tag{28}$$

where $X(s)$ is a variable to be controlled, $U_0(s)$ an external input, and $G_C(s)$ the transfer function of the compensator. The parameters of the compensators were selected experimentally so as to give the suitable frequency characteristics to the external input in each main control system (see [5] for the detail).

Experimental data are obtained in the non-rotation state of rotor. The results are shown for the axial and vertical motions which are supposed to interact each other from the model.

5.1 Frequency Responses

Frequency responses of the rotor motion were measured for a sinusoidal input with the amplitude of 0.5V, superimposed on the control input as in eq. (28). As is shown below, the displacements for this input are small: even the maximum of the conical motion is about 25 μm. This is due to the small external force generated by the actuators based on the single action control. The larger input give a larger motion, but it may lead to a nonlinear response.

The conical displacement is displayed down by 3dB (1.43=3.11 dB), for simplicity of comparison (the gain of the sensor is 1.43 times the others).

Figure 4 shows the gain responses to the input in the conical control system of the vertical direction. In the lower frequencies, the induced motion is lager in the axial direction than in the vertical translation as expected in the model. In the higher frequencies, however, an unexpected large translatory motion is induced.

The responses to the input in the axial control system are given in Fig. 5. The results are different from the preceding ones. The induced translatory motion is as large as the conical motion, which is not expected from the model. The induced motions have two peaks in the higher frequencies. The dent in the axial gain around 55Hz is considered due to the insufficient stiffness of the setup with the dent of the conical gain around 30Hz; however, it may not be reasonable to give the same reason for the rise in the induced motions around 45Hz.

For the axial and conical responses, the numerical results are compared with the experiments in [5] with a good

agreement except for the rise of the induced motion in the higher frequencies. Similar rise in the gain of the induced motions was reported also in [3]-[5] with the guess that the primary facotr is the problem of the hardware: the stiffness, the accuracy in manufacturing, *etc.* The conclusion is given in [6], however, that the cause is the interaction of the control force caused by the saturation of absolute inputs: the nonlinear effects based on the control saturation.

This idea gives a reasonable explanation for the above results. Of the absolute inputs, E_{11} saturates most easily in the lower limit because the bias input of about 1V leads to a smaller admissible increment for the lower limit of 0V than for the upper of 4V. From the assignment of the actual inputs, we see that this saturation is possible in the control of the axial and vertical-conical motions, more possible in the latter motion. It may be possible to suppose the effects of this saturation with the linearized input relations (12)-(16), *i.e.* the saturation of v_{11} affects the motions except for the radial-horizontal motions. Also we can see in the input relations that similar saturation of the upper part caused by the translatory motion control has no effect on the other control inputs: the effects are canceled. This was checked with the experiments.

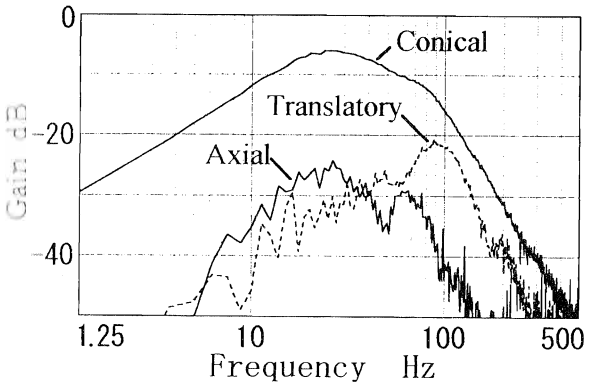

FIGURE 4. Frequency Gain-Responses to Conical Input

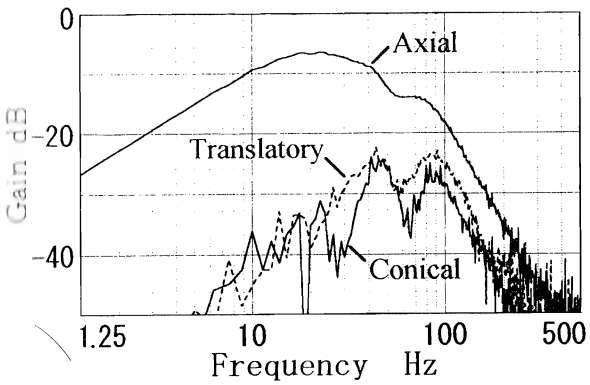

FIGURE 5. Frequency Gain-Responses to Axial Input

5.2 Responses to Axial Impact

To examine the characteristics with larger displacements, impact is given directly to the rotor into the axial direction; the impact into the conical direction is difficult because of the structure of the setup. The axial motion control is the single action as noted in the preceding section so that the transient responses make clear the properties of the single-action control as shown below.

Figure 6 give the result for an impulse moving the rotor away from the EMs working in the control. The motion in the other directions might be induced by the interacting control forces due to the saturation of the inputs. The rotor is attracted to the EMs in the approaching side when a larger axial displacement is given. The result for the opposite direction is shown in Fig.7, where the induced motion is much larger. In this case, with a larger displacement, the rotor moves down and touches the emergency bearing; thus, the allowable axial displacement is about one-third of the former case. The induced motions become larger with larger control gains.

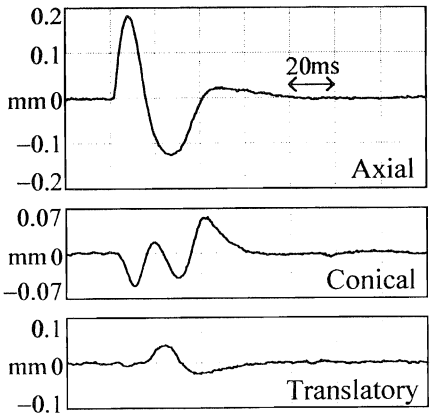

FIGURE 6. Responses to Axial Impact Moving Away from Working EMs

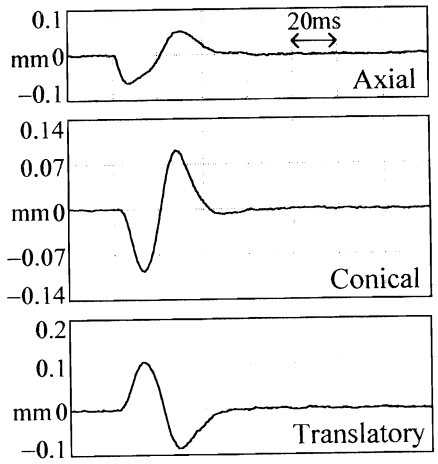

FIGURE 7. Responses to Axial Impact Moving Toward Working EMs

5.3 Control System with k=0

Setting k =0 in Fig. 3 simplifies the control system a little and gives a smaller input for the conical control. Figure 8 gives the frequency responses corresponding to Fig. 4 with the same control parameters. The induced axial motion is smaller than that in Fig.4 in the lower frequencies, but larger in the higher frequencies; this may be pure chance. The translatory motion omitted here is similar to

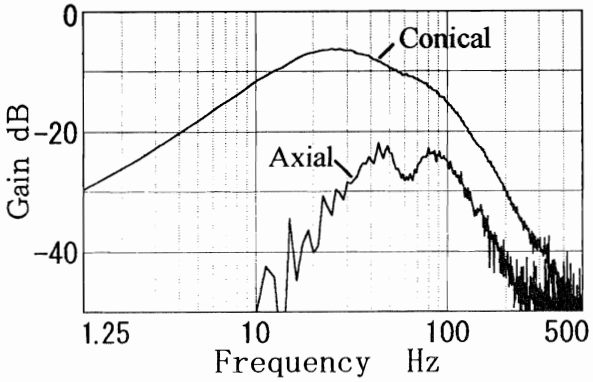

FIGURE 8. Frequency Responses to Conical Input with k=0

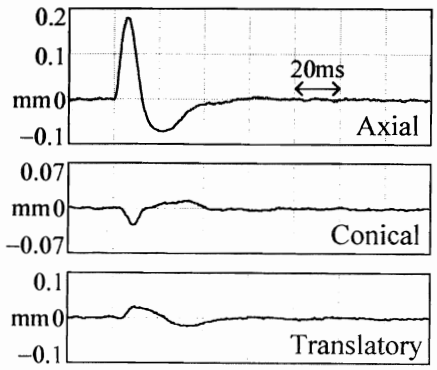

FIGURE 9. Responses to Axial Impact Moving Away from Working EMs with k=0

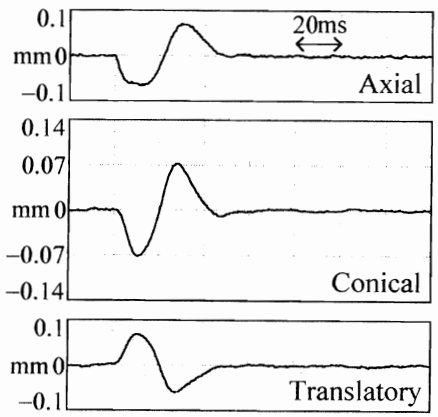

FIGURE 10. Responses to Axial Impact Toward Working EMs with k=0

that in Fig. 4 in the lower frequencies and a little larger in the higher frequencies: near to the axial response. The results corresponding to Fig. 5 are similar to those. Thus, omitting k affects only the induced axial motion in the lower frequencies; this confirms the role of k stated above. The transient responses corresponding to Figs. 6 and 7 are given in Figs. 9 and 10, respectively. The interaction is much smaller in the direction moving away from the working EMs, and is a little smaller in the opposite direction. These results may suggest the effects of interacting control with the input saturation.

6. CONCLUSIONS

An approximate decoupling control system was designed with five electromagnets for the symmetric cone-shaped bearing system supporting a symmetric rotor in the horizontal direction. The control action is not push-pull but individual with a pair of electromagnets in the axial and vertical control axes. The square-root compensation is applied for the linearization of these single-action control systems. The experimental results showed the usefulness of the design method, but also made clear the properties of the single action of the control, the weak points. Some improvements may be possible with an interacting control scheme; but the single control action may be inherent in saving the actuators.

REFERENCES

1. Inoue,M., and Shimomura,T., Development of a Magnetic Momentum Wheel with Skewed Electromagnets, Proc. of the 10th Inter. Workshop on Rare-Earth Magnets and Their Applications, Kyoto, Japan, 1989.
2. Fukata, S., Linearized Model and Control Systems of Active Magnetic Bearings with Magnet Cores in the Shape of a Cone, Trans. JSME, Vol. C-58, No.551, pp.2081-2088, 1992. (in Japanese)
3. Fukata, S., and Kouya, Y., Dynamics of Active Magnetic Bearings with Magnet Cores in the Shape of a Cone, Proc. of the 3rd Int. Symp. on Magnetic Bearings, Alexandria, Virginia, 1992.
4. Fukata, S., Dynamics of Magnetic Bearings Composed of Six Electromagnets in the Shape of a Cone, Trans. JSME, Vol. C-59, No.568, pp.3765-3772, 1993.(in Japanese)
5. Fukata, S., and Matsuoka, S., Approximate Decoupling Control System and Dynamics of Magnetic Bearings Controlled by Five Electromagnets in the Shape of a Cone, Trans. JSME, Vol. C-60, No.573, 1994. (in Japanese)
6. Fukata, S., Control System and Dynamics of Cone-Shaped Magnetic Bearings Supporting a Vertical Rotor, Proc. of Okinawa Symp. of JSME Kyushu, Okinawa, Japan, 1994. (in Japanese)